Hybrid Pulsating Heat Pipe for Space Applications with Non Uniform Heating Patterns: Ground and Microgravity Experiments

D. Mangini[1], M. Mameli[2] , D. Fioriti[2], S. Filippeschi[2], L. Araneo[3], M. Marengo[4]

[1]*Faculty of Engineering, University of Bergamo, Dalmine, Italy*
[2]*DESTEC, University of Pisa, Pisa, Italy.*
[3]*Faculty of Engineering, Polytechnic of Milan, Milan, Italy*
[4] *School of Computing, Engineering and Mathematics, University of Brighton, England*

Abstract

A hybrid Loop Thermosyphon/Pulsating Heat Pipe named Space Pulsating Heat Pipe (SPHP) is tested both on ground and in hyper/micro-gravity conditions during the 63rd ESA Parabolic Flight Campaign. The device, partially filled up with FC-72 (50% Filling Ratio), is made of an aluminum tube (Inner/Outer Diameter 3 mm/5 mm) bent into a planar serpentine with five curves at the evaporator zone. A transparent section closes the loop in the condenser zone, permitting the fluid flow visualization. Each of the five heaters, mounted alternatively on the branches, just above the curves, is controlled independently, in order to test different heating distributions. The device is tested at different total heat inputs (50 W, 70 W and 90 W), both on ground and in hyper/micro gravity conditions. Data are collected by recording the heat power provided to each heater, the tube wall temperatures, the fluid pressure and fast speed images up to 200 fps are also recorded in the transparent section. An image processing software is developed in order to calculate the bubble flow velocity. On ground, where the device acts like a thermosyphon, the non-uniform heating promotes the fluid net circulation in a preferential direction, stabilizing the operation of the device and thus increasing the thermal performance with respect to the homogeneous heating. The parabolic flight tests point out a working mode in microgravity for such SPHP: the sudden absence of buoyancy force, activating an oscillating slug/plug flow regime, allows the device to work also without gravity assistance. It was found that particular heating distributions can shorten the stop-over periods observed when the device is uniformly heated up, stabilizing a pulsating two-phase flow motion when the gravity field is absent.

Keywords: Thermosyphon; Pulsating Heat Pipe; Microgravity; Flow Visualization.

1. INTRODUCTION

The continue miniaturization of electronics in space thermal control systems, coupled with their ever increasing performance year by year, has resulted in a dramatic rise in the amount of heat generated per unit volume both on ground and in space thermal control management. In the last decades, the role of the two-phase heat transfer devices achieve more and more importance because of their compactness, lightweight, high performance and reliability. The Capillary Pumped Loops (CPL) and Loop Heat Pipes (LHP) have been already successfully utilized in a variety number of space missions for their peculiar advantages [1]. Utilizing a "wick" capillary inner structure, the CPL and LHP are able to transport heat along tortuous and longer paths in a very efficient way, thus decreasing the temperature gradient between the heated and the cooled zone, too. Nevertheless, the "wick" structure is not only the most expensive element in the system, but it is also the most difficult one to design and to characterize.

In order to decrease the effectiveness to cost ratio, Akachi [2] invented a new kind of passive wickless capillary two-phase loop named Pulsating Heat Pipe (PHP). The PHP consists simply in a capillary tube bended in order to have U-turns with alternated heated and cooled zones. The device is firstly evacuated and then partially filled-up with the working fluid. The capillary dimensions of the tube, making the surface tension forces slightly predominant with respect to the body forces, creates an alternation of "liquid slugs" and "vapor bubbles" inside the device. The expansion of the vapor plugs in the heated zone, pushing the adjacent fluid in the condenser zone, permits to release heat in the cooled zone. To the contrary, in the cooled zone, the condensation of the vapor bubbles permits to recall more fluid from the evaporator. These continue phase changes, establishing a pulsating and chaotic two-phase flow motion [3], are the principal responsible of the fluid motion in the device [4]. Thanks to the capillary dimension of the diameter and the peculiar slug/plug flow motion, the PHP has the relevant advantage, in comparison to other passive heat transfer devices such as Thermosyphons (TS) or Heat Pipes (HP), to work also if it is not gravity assisted (i.e. for space applications [5] or when horizontally oriented on ground [6]). The correct choice of the inner diameter (ID) dimensions is crucial to guarantee a slug/plug

*Corresponding author: mauro.mameli@ing.unipi.it, Phone: +39 050 2217166.

flow motion. The Bond criterion is usually adopted by the PHP community to define the confinement diameter:

$$d_{cr,Bo} = 2\sqrt{\sigma/g(\rho_l - \rho_v)} \quad (1)$$

However, after the start-up, inertial and gravitational effects plays an important role: for this reason, it is mandatory also to take into account the inertial and the gravitational effects. The dynamic limits based on the Weber number:

$$d_{We} = 4\sigma/\rho_l U_l^2 \quad (2)$$

and on the Garimella number:

$$d_{cr,Ga} = \sqrt{(160\mu_l/\rho_l U_l)\sqrt{\sigma/g(\rho_l - \rho_v)}} \quad (3)$$

are therefore more suitable to define the limit for space applications, as thoroughly explained by Mameli et al. [7], even if further experimental validations are necessary. In order to provide some order of magnitude, the Table 1 shows the confinement diameter both on static and dynamic conditions both in earth-gravity and in microgravity for FC-72 at 20°C considering an average fluid velocity of 0.1 m/s:

Table 1. Confinement diameters for FC-72 at 20 °C both in static and dynamic conditions, on ground and micro-gravity conditions.

FC-72 at 20 °C	$D_{cr,Bo}$ [mm] (static)	D_{Ga} [mm] with U_l=0.1 m/s
Earth gravity: g=9.81 m/s^2	1.68 mm	0.75 mm
Microgravity: g=0.01 m/s^2	52.88 mm	4.23 mm

Taking also into account the inertial effects, it is possible to design a PHP with an ID diameter slightly higher than the critical one able to guarantee a slug/plug flow motion. This concept has recently been demonstrated by Mangini et al. [8] by means of parabolic flights. This device is called by the authors Pulsating Heat Pipe only for Space (SPHP) and it opens the frontiers to a new kind of thermal devices able to work as a Multi-Evaporator Loop Thermosiphon in presence of gravity, and as a PHP in microgravity conditions. Following this idea, other experimental attempts were performed by Creatini et al. [9], testing a similar SPHP onboard the ESA REXUS Sounding Rocket. Unfortunately the de-spin system of the rocket malfunctioned and the consequent centrifugal acceleration did not allow to reach the capillary regime. Nevertheless, looking to the results obtained testing the SPHP by Mangini et al., even if it is demonstrated that the device works as a PHP in microgravity, the slug/plug motion has an "intermittent" behavior when gravity acceleration approaches 0 m/s^2. When the SPHP is not gravity assisted, vigorous pulsations are followed by prolonged stop-overs periods. In such periods, both the liquid and the vapor phase, completely stopped, are not able to deliver heat from the heated to the cooled zone, with a negative impact on the heat exchange: temperatures at the evaporator zone exhibits an ever-increasing trend.

The aim of this work is to prove that, positioning non-symmetrically the heating elements in the heated zone and providing to the SPHP appropriate heating distributions it is possible to:

- stabilize the fluid motion in a preferential direction on ground, improving its thermal performance, when the device is gravity assisted;
- reduce stop-over periods in microgravity, permitting to establish a slug/plug flow motion that continuously oscillate also when the gravity field is absent.

A PWM electronic system is implemented, allowing to control independently five heating elements positioned at the evaporator, so as to vary the heating distribution along the evaporator.

2. EXPERIMENTAL APPARATUS AND PROCEDURE

The actual SPHP is an aluminum tube (I.D./O.D. 3.0 mm/5.0 mm; global axial length: 2550 mm) bended into a planar serpentine with five turns at the evaporator zone (all curvature radii are 7.5 mm), as shown in Fig. 1a. Two "T" junctions derive two ports at each side: one hosts a pressure transducer (Kulite®, XCQ-093, 1.7 bar abs.), while the second one is devoted to the vacuum and filling procedures. The device is partially filled-up with FC-72 (FR = 0.5, corresponding to 8.3 ml). Sixteen "T" type thermocouples (with a bead diameter of 0.2 mm and an accuracy of ± 0.3 K) are fixed at the PHP external tube wall: ten are located in the evaporator zone, while other six in the condenser zone. The ambient temperature is monitored by means of PT 100 sensor (PT 100 Class B sensor RS®). A glass tube (axial length: 50 mm), positioned between the two "T" junctions allows fluid flow visualization and closes the loop. A compact camera (Ximea®, MQ013MG-ON objective: Cosmicar/Pentax®

C2514-M) is positioned behind the SPHP by means of an aluminum plate, allowing to record up to 200 fps images of the flow evolution inside the glass tube with a resolution of 1280x170 pixel (25 pixel/mm). A low vapor pressure epoxy (Varian Torr Seal®) is utilized to glue the "T" junctions, the edges of the device and the glass tube all together, guarantying also excellent sealing.

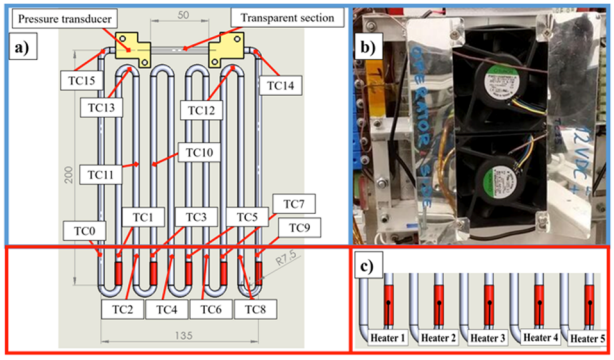

Fig. 1. a): thermocouples location along the SPHP tube, b) the condenser zone; c) the 5 heating elements, mounted alternatively just above the U-turns at the evaporator zone.

Five heating elements (Thermocoax® Single core 1Nc Ac, 0.5 mm O.D., 50 Ω/m, each wire is 720 mm long) are wrapped just above the U-turns at the evaporator zone, covering a tube portion of 20 mm each one. The peculiar position of the heaters is highlighted in Fig. 1c. The power per each heater is regulated with the PWM technique at 10 Hz operated by the control system. Five independent MOSFET relays PVG612A work as interfaces between the control system and the power side permitting to heat up the device with different heating distributions at the evaporator. The power supply (MW RSP-320 series) provides an electric power input up to 160 W, corresponding to a wall to fluid radial heat flux up to 17 W/cm^2, with a maximum error of 4.7%. Pseudo-steady state condition can be reached in approximately 3 minutes, due to the low thermal inertia of the heating system and the device. The condenser section is 165 mm long and it is embedded into a heat sink, which is cooled by means of two air fans (Sunon® PMD1208PMB-A), as shown in Fig. 1b. Gravity variations during each parabola are detected by means of a three-axis g-sensor (Dimension Engineering®, DE-ACCM3d). The device, the heating and the cooling system, all the sensors (thermocouples, PT100, pressure transducer and g-sensor) as well as the visualization system are placed on a beam structure by means of four anti-vibration bushes.

Firstly, the SPHP is vacuumed by means of an ultra-high vacuum system (Varian® DS42 and TV81-T) down to 0.3 mPa and then it is partially filled up with the working fluid (FC-72) with a volumetric ratio of 0.5 ± 0.03 and sealed by means of tin soldering. The fluid itself had been previously degassed within a secondary tank, by continuous boiling and vacuuming cycles as described by Henry et al. [10].

A data acquisition system (NI-cRIO-9074®, NI-9264®, NI-9214®, 2xNI-9205®, NI-9217®, NI-9472®) records the output of the thermocouples (at 10 Hz), the pressure transducer (at 200 Hz) and the g-sensor (at 5 Hz). The high-speed camera is connected to an ultra-compact PC (NUC® Board D54250WYB) able to store images up to 200 fps. The video, synchronized with the pressure signal, is recorded for 80 seconds during each parabolic maneuver and for 30 seconds during tests on ground after reaching steady state conditions. On flight, the movie starts approximately ten seconds before the maneuver and stopping around ten seconds after the second hyper-gravity period. The bubble velocity is after measured with an open source PIV software [11] partially modified to detect the vapor phase motion along the transparent section. Velocities are measured at 80% of the axial length of the tube, 8 mm from the pressure transducer position.

The experimental parameters are:

- The total heat input levels, 50 W, 70 W or 90 W which is the sum of all the power levels provided by each of the five heaters.
- The different heating distributions among the five heaters at the evaporator zone.
- The gravity field: normal gravity (1g) during the test on ground and during the straight flight trajectory; hyper-gravity (1.8g) before and after the parabola during the ascending and descending maneuvers (duration: 20-25 s each); microgravity during the parabola (duration: 20-21 s).

3. EXPERIMENTAL RESULTS

In this section, results are presented in terms of temperatures and pressure temporal evolutions, while the two-phase flow images recorded both during ground tests and the entire parabola performed are post-processed to find the bubbles velocity during the entire movie.

3.1 Ground tests

The device has been thermally characterized on ground in bottom heated mode with different heating distributions utilizing three different levels of global heat power input: 50 W, 70 W and 90 W. All the heating configurations are kept constant for at least 15 minutes. The thermal performance of the device is standardly calculated by means of the Equivalent Thermal Resistance (R_{eq}):

$$R_{eq} = \frac{\overline{\Delta T}_{e-c}}{\dot{Q}} \quad (4)$$

where $\Delta T_{e\text{-}c}$ is the difference between the evaporator and the condenser average temperatures in the pseudo-steady state and $\dot{Q}$ is the effective global heat power input provided to the device in the evaporator zone. In the heated branches (up-headers, highlighted with red arrows in Fig. 2), the expansions of vapor bubbles push liquid batches to the condenser, while the refreshed liquid and vapor phase can easily return to the evaporator thanks to gravity by the adjacent branches (down-comers, highilighted with blue arrows in Fig. 2), promoting a two-phase flow circulation in a preferential direction, as already demonstrated [12].

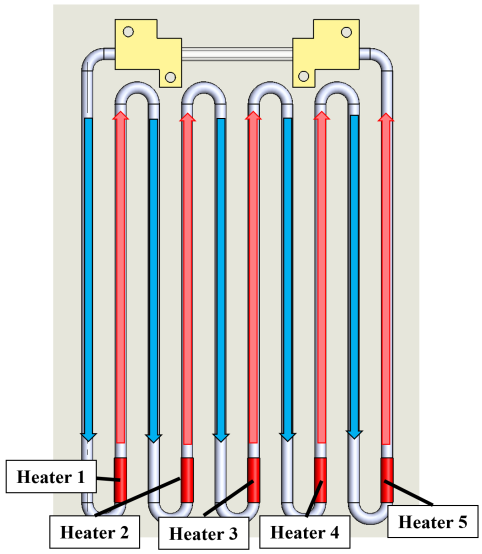

Fig. 2. Non-Symmetric heater layout and flow circulation: up-headers highlighted with red arrows; down-comers highlighted with blue arrows.

The peculiar position of the heaters creates also a non-symmetric hydrodynamic configuration. The U-turns between the down-comers and the heating elements, representing an important concentrated pressure loss for a two-phase flow [13], allows the liquid batches to easily reach the condenser from the straight up-headers. Results show that the five independent heaters, supplying different power levels, generate an overall imbalance in the system able to promote a net fluid circulation. For the 50 W case, R_{eq} continues to decrease up to 8.7% from the Configuration 2 to the Configuration 5 with respect to the uniform heating configuration (Fig. 3). This is due to a better stabilization of the two-phase flow motion: increasing the heat power input provided by the heater 5, the continue bubble expansions push the liquid batches more vigorously in the horizontal section of the condenser. Nevertheless, increasing excessively the amount of power provided to the Heater 5 creates an unstable thermo-fluid behavior (Configuration 6): the high RMS value (11,8%) in the R_{eq} plot points out continue oscillations of the temperatures both at the evaporator and at the condenser zone. Increasing the heat power at both of the lateral up-headers, the R_{eq} decreases of 4.1% with respect to the homogeneous heating distribution. In such configuration, the larger heat exchange area in the condenser zone is able to dissipate a higher amount of power supplied by the lateral heaters, increasing consequently the thermal performance.

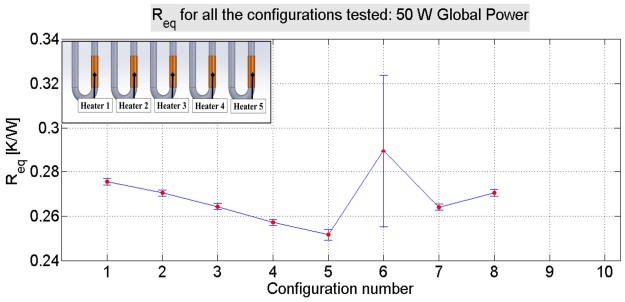

Configuration	Heater1	Heater2	Heater3	Heater4	Heater5
1	10 W	10 W	10 W	10 W	10W
2	9 W	9 W	9 W	9 W	14 W
3	6 W	8 W	10 W	12 W	14 W
4	4 W	7 W	10 W	13 W	16 W
5	2 W	6 W	10 W	14 W	18 W
6	6 W	6 W	6 W	6 W	26 W
7	14 W	8 W	6 W	8 W	14 W
8	12 W	8 W	10 W	8 W	12 W

Fig. 3. R_{eq} values for the configurations tested on ground providing a global power of 50 W.

Similar results are obtained with a global heat power input at 70 W. Again, increasing continuously the power supplied from the heater 1 to the heater 5, the R_{eq} decreases with respect to the homogeneous heating of more than 4%. Additionally, the bubble velocities is calculated when it is supplied a homogeneous heating (Fig. 4) and a non-uniform one (Fig. 5). A sequence of images, (30 seconds at 200 fps), starting 28 minutes after each heat input power variation in order to have reached pseudo-steady state conditions, is after post-processed to find bubble velocity between each frame recorded. As a convention, the velocity of the bubbles has positive values when the motion is detected from the right to the left of the transparent section; negative in the opposite case. For instance, if the bubble velocity has always higher values than 0 m/s, it means that there is a net circulation in a preferential direction from the right to the left.

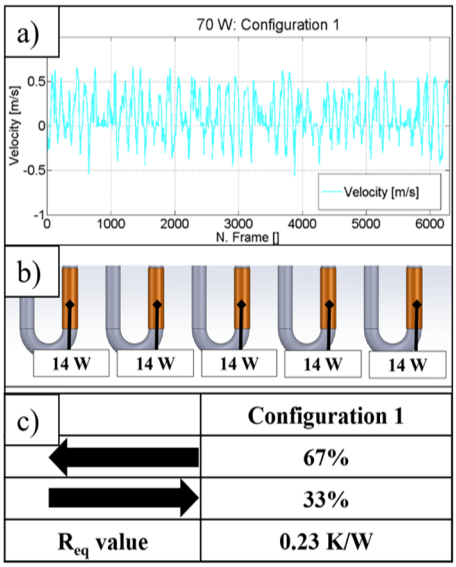

Fig. 4. a) Bubble velocity when the device is heated up uniformly; b) the heating configuration provided; c) Bubble direction and R_{eq} value.

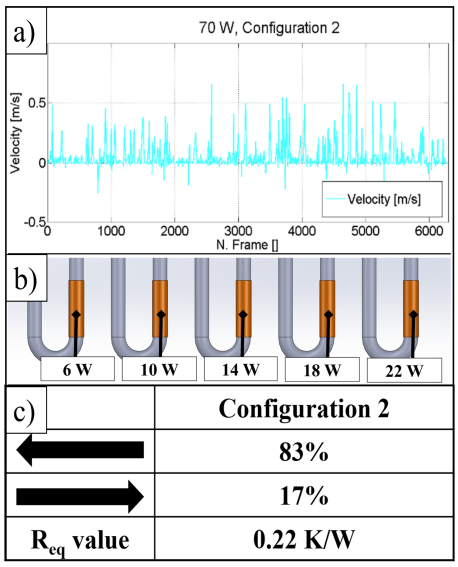

Fig. 5. a) Bubble velocity when the device is heated up non uniform; b) the heating configuration provided; c) Bubble direction and R_{eq} value

The velocity measurements point out an improvement of the circulation in a preferential direction from the right to the left when the SPHP is non-uniformly heated up. In such configuration the bubbles move towards the transparent section for the 83% of the time (Fig. 5); while when the device is uniformly heated up, only for the 63% of the time (Fig. 4). The circulation in a preferential direction has a positive impact on the overall performance: the R_{eq} value decreases of 0.1 K/W in the non-uniform case.

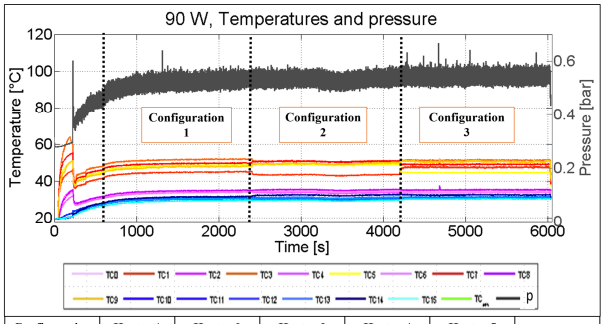

Configuration	Heater 1 [W]	Heater 2 [W]	Heater 3 [W]	Heater 4 [W]	Heater 5 [W]	Req [K/W]
1	18	18	18	18	18	0,21
2	14	16	18	20	22	0,2
3	24	16	10	16	24	0,2

Fig. 6. Temperatures and pressure recorded for all the configurations tested on ground utilizing a global power of 90 W.

Heating up the device with a global power input of 90 W, the R_{eq} tends to 0.2 K/W for all the configurations tested. No significant improvements in terms of performance are detectable changing the heating distribution for such global power: it is sufficient the non-symmetric position of the heaters to stabilize the two-phase flow motion in a preferential direction.

As it is visible from the Fig. 6, the temperatures both at the evaporator and at the condenser zone are stable for all the heated configurations. As a conclusion, the non-uniform heating distribution has a positive impact on the performance of the SPHP especially for the lower global power tested. Increasing the global-power, the only non-symmetric position of the heaters is sufficient to provide a stabilization of the flow motion.

3.2 Flight tests

Microgravity experiments were carried out aboard the ESA/Novespace Airbus A300, during the 63rd ESA PF campaign. In each flight, a total of 31 parabolic trajectories were performed. Three days of flight are provided to carry out experiments. In every day of flight, the first parabola (called parabola zero) is followed by six sequences, each consisting of five consecutive parabolic maneuvers [14]. All sequences are separated by 5 minutes of interval at earth g-level. In the three days of flight, tests are performed varying the distribution of the heat power input at the evaporator zone. The different heat power distributions at the evaporator zone tested are changed in the five minutes pause at earth-gravity level between one set of parabola to the next one, to allow reaching a pseudo-steady state conditions before the beginning of the next parabolic trajectories. All the different heat power

input distributions are kept constant for the entire set of five parabola to ensure repeatability. The procedure described above is followed and repeated in all the three days of flight. The device is tested in Bottom Heated Mode.

During microgravity periods, the sudden absence of the buoyancy forces allows the surface tension force to form menisci, permitting the vapor phase to fill-up completely the tube section and making the device to work as a PHP (Fig. 7).

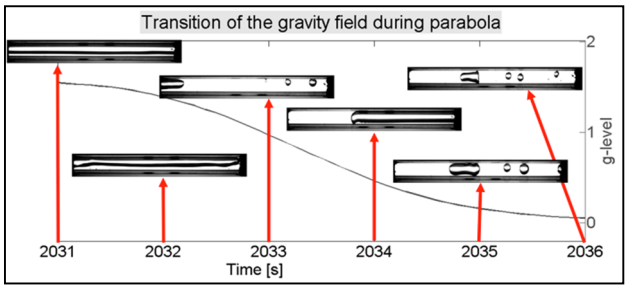

Fig. 7. Gravity field transition from hyper to micro-gravity: activation of a slug/plug flow regime.

In microgravity, when each of the five heaters dissipates 10 W (Fig. 8a), the thermo-fluid behavior is "intermittent": oscillating periods, in which the pressure signal exhibits fluctuations (green sections, Fig. 8b) and slug/plug flow motion is observable in the transparent section, are followed by prolonged stop-over (red sections in Fig. 8b and in Fig. 8c). During stop-over periods, the pressure is nearly constant, while the bubbles in the transparent section are stopped at the same position. This stagnant situation has a negative impact on the heat exchange. As shown in Fig. 8b, during each stop-over, the temperatures at the evaporator exhibit an ever-increasing trend. When the fluid starts again to oscillate, the temperatures stabilize, proving the importance of the flow motion on the heat exchange.

The stop-over periods do not occurs providing to the SPHP a peculiar non-uniform heating distributions (Fig. 9a). Increasing the power at the lateral up-headers and decreasing it at the center, the pressure signal fluctuates continuously in microgravity (Fig. 9b), while the bubble velocity measurements point out an oscillating flow (Fig. 9c). The constant flow oscillations have a positive effect also in the heat exchange: even if the lateral up-headers dissipates an heating power 40% higher than the uniform case, the maximum temperatures approaches 60 °C at the end of the micro-gravity period. Increasing the heat power inputs at the lateral up-headers, the larger heat exchange area at the condenser permits to dissipate a higher amount of power.

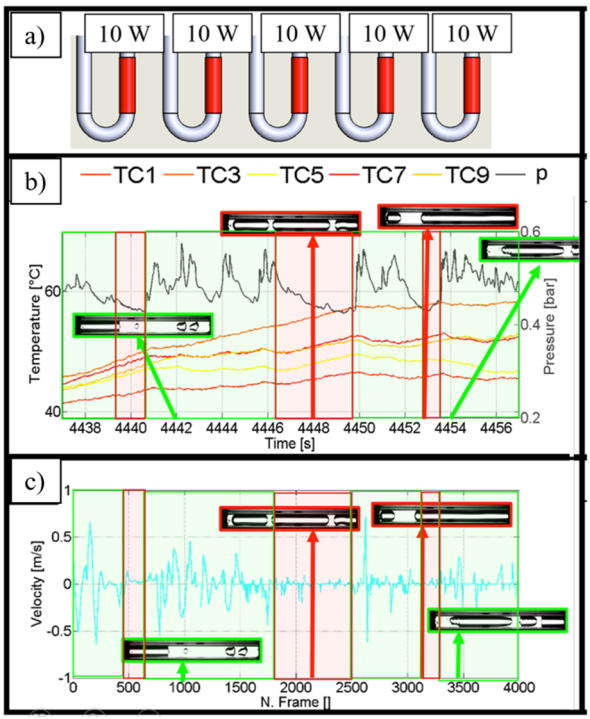

Fig. 8. a) Power supplied by the five heating elements: uniform heating pattern; b) Temperatures at the evaporator and pressure during microgravity; c) Bubble velocity measured in microgravity.

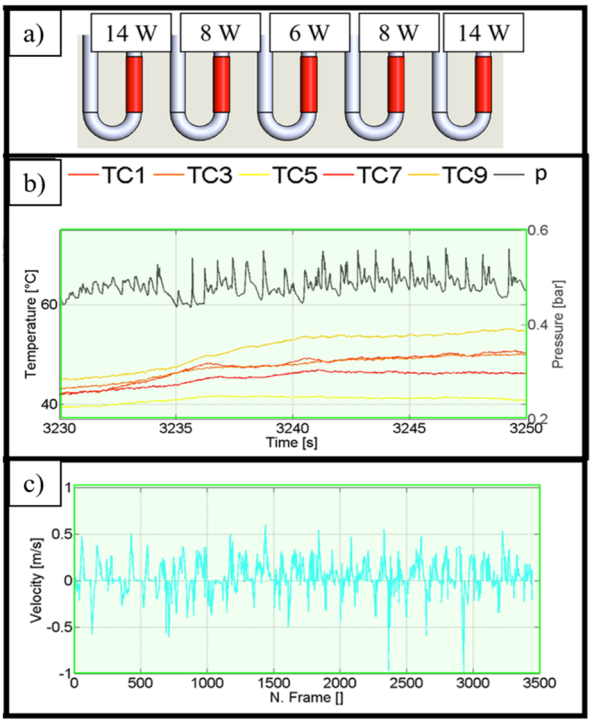

Fig. 9. a) Power supplied by the five heating elements: non-uniform heating pattern; b) Temperatures at the evaporator and pressure during microgravity; c) Bubble velocity measured in microgravity.

When the device works as TS, the gravity certainly assists the flow motion, giving a net contribution to the fluid momentum. The gravity force is like an interconnection component between the different up-headers, permitting to the liquid phase to fall down through the down-comers and refreshing continuously the evaporator. As a consequence, even if the up-headers are heated up with non-uniform power levels, the temperatures at the evaporator resides in a narrow range (First Hyper-gravity period in Fig. 10): the fluid circulation keeps constant each ones. Nevertheless, in microgravity, the sudden absence of a gravity field "disconnects" all at once the five heating elements: in such condition, the expansions and contractions of the vapor phases are the principal responsible of the flow motion. The non-heated branches are not anymore "down-comers", since in microgravity the liquid phase returns at the evaporator only if it is properly pushed by the phase change phenomena. Therefore, after the transition from hyper-gravity to microgravity the evaporator temperatures tend to spread in a wider range, from 35 °C to 70 °C, depending on the heating power provided to each element (Microgravity period in Fig. 10).

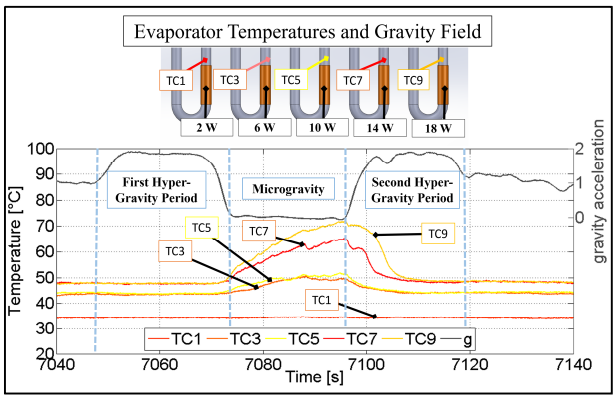

Fig. 10. Temperature evolution at the evaporator during parabola.

As soon as the second hyper-gravity is achieved, the sudden return of the gravity field, linking again the heated zone and permitting to the liquid phase to be pushed again in the heated zone, decreasing immediately all the temperatures at the evaporator.
Providing to the SPHP a global heat power of 70 W, again, an intermittent working mode is recognizable when the SPHP is uniformly heated up (Fig 11): stop-over periods, that last up to six seconds (highlighted with a red rectangle in Fig. 11a), are followed by sudden peaks in terms of pressure. Increasing the power value at the lateral up-headers and decreasing it at the center, stop-over periods are another time limited (Fig. 11b): the pressure signal oscillates continuously, pointing out a continue flow pulsating slug/plug motion.

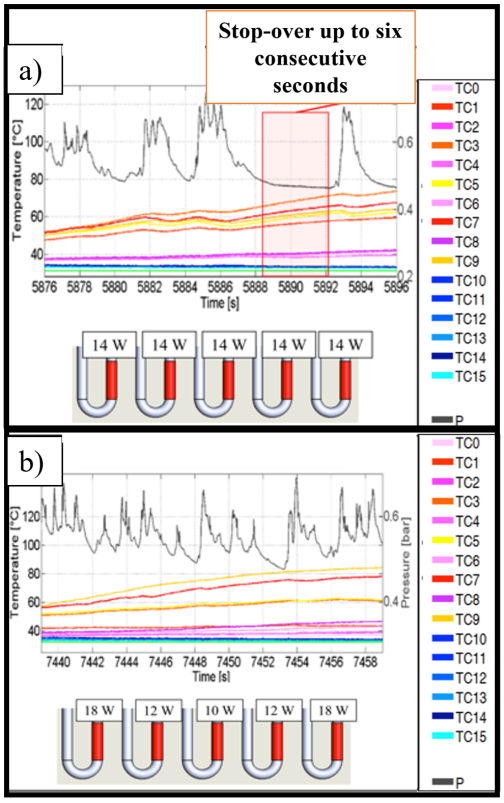

Fig 11. Pressure and temperatures during microgravity providing a global power of 70 W in a) uniform heating and b) non-uniform heating configuration.

Increasing the global heat power input up to 90 W, also the non-uniform heating distribution shown in Fig. 12 stops the flow motion during the last seconds of micro-gravity.

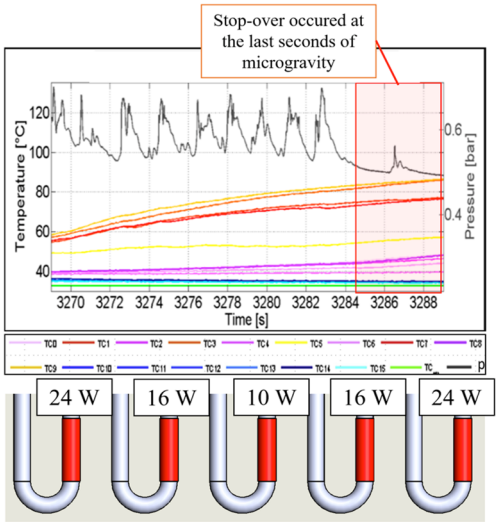

Fig. 12. Non-uniform heating distribution tested with a global power of 90 W: pressure and temperatures in microgravity.

The pressure does not oscillate, while the temperatures at the evaporator highlight an ever-increasing trend, reaching 95 °C at the end of the 20 seconds of microgravity, synonymous of dry-out occurrence. In such configurations, the lateral heating elements dissipate up to 24W, corresponding to a local heat flux of 13 W/cm^2.

4. CONCLUSIONS

A novel concept of hybrid closed loop Thermosyphon/Pulsating Heat Pipe with an inner diameter slightly higher than the static threshold on ground, is tested both at Earth g-level and in hyper/microgravity conditions during the 63rd ESA PFC. The device is made by an aluminum tube, bended in order to have five U-turns at the evaporator, partially filled with FC-72. Five heating elements, mounted just above the U-turns at the evaporator zone, are controlled independently, allowing to test different heating configurations at the evaporator. On ground the device works as a closed loop two-phase Multi-Evaporator Thermosyphon. Results point out that, heating up the device non-uniformly at the evaporator, a circulation in a preferential direction is established, with an improvement of the overall thermal performance, especially for the lower heating power tested. In microgravity conditions, the sudden absence of the buoyancy force permits to activate a typical PHP oscillating slug/plug flow. The non-heated branches in microgravity are no more "down-comers", since the liquid phase can not returns in the heated zone thanks to a gravity field. As a consequence, the different heated branches are more independent between each other. Nevertheless, heating up the device non-uniformly has a beneficial impact also in microgravity. The homogeneous heating distribution causes an intermittent working mode when the device is not gravity assisted: stop-over periods are spaced out by vigorous two-phase flow oscillations. The non-uniform heating distribution, establishing a pulsating motion also when gravity is absent, decreases abruptly the stop-over periods. Finally, a large amount of experiments was done in the last decades to explore the effect of the reduced gravity field both for pool boiling and flow boiling conditions [15]. All the results show that the CHF in microgravity is significantly smaller with respect the values obtained on hearth for pool boiling: the sudden absence of buoyancy forces, making more difficult the bubble departure from the heated zone, reduces the working range in terms of maximum heat fluxes. Flow boiling, especially when the flow inertia is predominant, constitutes a practical and effective means to precluding this stagnant situation: the liquid inertia extracts bubbles away from the heated wall, providing a path for bulk liquid to fill up again the heated wall. Nevertheless, very few studies have been devoted exclusively to flow boiling CHF in reduced gravity. Results obtained for the highest heat power input point out that in the SPHP, even if the oscillating slug/plug motion in microgravity is able to exchange heat from the heated to the cooled zone, when microgravity occurs, the CHF decreases down to 13 W/cm^2. To prove it, further experimental data in prolonged microgravity conditions are necessary.

AKNOWLEDGMENTS

The present work is carried forward in the framework of two projects: the Italian Space Agency (ASI) project ESA_AO-2009 and the ESA MAP Project INWIP, coordinated by Prof. Raffaele Savino. We would like to thank Ing. Battaglia for his administrative support; the NOVESPACE team in Bordeaux; Dr. Olivier Minster and Dr. Balazs Toth for their interest and support to the PHP activities.

NOMENCLATURE

Bo : Bond Number
d : Diameter (m)
FR : Filling Ratio
g : Gravity acceleration (m/s^2)
Ga : Garimella Number
T : Absolute temperature (°C)
Q : Heat Power Input (W)
R_{eq} : Equivalent Thermal Resistance [K/W]
Re : Reynolds Number
U : Fluid Velocity [m/s]
We : Weber Number
μ : Dynamic Viscosity [Pas]
ρ : Density [kg/m^3]
σ : Surface Tension [N/m]
CHF: Critical Heat Flux [W/cm^2]

REFERENCES

[1] G. Gilmore, *Spacecraft Thermal Control Handbook*, Fundamental Technologies, The Aerospace Press, El Segundo California (2002).

[2] H. Akachi, Structure of a heat pipe. US Patent 4,921,041, (1990).

[3] Zhang, Y., Faghri, A., Advances and unsolved issues in pulsating heat pipes, *Heat Transfer Engineering*, 29 (2008), 20-31.

[4] Khandekar, S., Groll, M., Charoensawan, P., Terdtoon, P., Pulsating Heat Pipes: Thermo-fluidic Characteristics and Comparative Study with Single Phase Thermosyphon, *Proc. of 12th International Heat Transfer Conference*, Grenoble, France (2004), 459-464.

[5] Gu, J., Kawaji, M., Futamata, R., Effects of gravity on the performance of pulsating heat pipes, *Journal of Thermosphysics and Heat Transfer*, 18 (2004) 370-378.

[6] Charoensawan, P., Terdtoon, P., Thermal performance of horizontal closed-loop oscillating heat pipes, *Applied Thermal Engineering*, 28 (2008), 460-466.

[7] Mameli, M., Araneo, L., Filippeschi, S., Marelli, M., Testa, R., Marengo, M., Thermal performance of a closed loop pulsating heat pipe under a variable gravity force, *International Journal of Thermal Science*, 80 (2014), 11-22.

[8] Mangini, D., Mameli, M., Geourgoulas, A., Araneo, L., Filippeschi, S., Marengo, M., A pulsating heat pipe for space applications: Ground and microgravity experiments, *International Journal of Thermal Sciences*, 95 (2015) 53-63.

[9] Creatini, F., Guidi, G.M., Belfi, F., Cicero, G., Fioriti, D., Di Prizio, D., Piacquadio, S., Becatti, G., Orlandini, G., Frigerio, A., Fontanesi, S., Nannipieri, P. Rognini, M., Morganti, N., Filippeschi, S., Di Marco, P., Fanucci, L., Baronti, F., Mameli, M., Manzoni, M. Marengo, M., Pulsating Heat pipe Only for Space (PHOS): results of the REXUS 18 sounding rocket campaign, *Journal of Physics: Conference Series 655* (2015).

[10] Henry, C.D., Kim, J., Chamberlain, B., Heaters size and aspect ratio effects on sub-cooled pool boiling heat transfer in low-g, *Proc. of 3rd International Symposium on Two-Phase Flow Modeling and Experimentation* Pisa, Italy, (2004).

[11] Taylor, Z.J., Gurka, R., Kopp, G.A., Liberzon, M., Long-Duration Time-Resolved PIV to Study Unsteady Aerodynamics, *Instrumentation and Measurement, IEDD Transactions*, 59 (2010) 3262-3269.

[12] Mameli, M., Mangini, D., Vanoli, G.F., Araneo, L., Filippeschi, S., Marengo, M., Multi-Evaporator Closed Loop Thermosyphon, *Proc. of 7th European-Japanese Two-Phase Flow Meeting*, Zermatt, Switzerland (2015).

[13] Da Silva Lima, R., Thome, J.R., Two-phase flow patterns in U-bends and their contiguous straight tubes for different orientations, tube and bend diameters, *International Journal of Refrigeration*, 35 (2012) 1439-1454.

[14] Novespace A300 Zero-G Rules and Guidelines, Paris, France (2009).

[15] Konishi, C., Mudawar, I., Review of flow boiling and critical heat flux in microgravity, *International Journal of Heat and Mass Transfer*, 80 (2015), 469-493.